Supporting information

Privileged zeolitic sites for humid CO_2 adsorption: K^+ in double eight-membered rings

Hwangho Lee *[a], Shu Hikima [b], Ryohji Ohnishi [b], Takahiko Takewaki [b], and Alexander Katz *[a]

[a] Department of Chemical and Biomolecular Engineering, University of California, Berkeley, California 94720, United States
[b] Mitsubishi Chemical Corporation, Science and Innovation Center, Aoba-ku, Yokohama 227-8502, Japan

Method

Zeolite synthesis

RHO zeolite was synthesized as described in previous literature.[1-2] Crown ether (18-crown-6), Cs-OH solution (50 wt.%) and NaOH were dissolved in deionized water. Then, sodium aluminate ($Na_2O{\cdot}Al_2O_3{\cdot}3H_2O$) was added to the solution, being stirred until it becomes clear. Colloidal silica (Ludox, AS-40) was added to the clear solution, and the final solution was aged at room temperature for 24 h. The final gel composition of the solution was 1.8 Na_2O: 0.3 Cs_2O:Al_2O_3:10 SiO_2:0.5 18-Crown-6:100 H_2O. After transferring the solution to a Teflon-lined stainless-steel autoclave, hydrothermal synthesis was performed at 125 °C for 3 days while rotating the autoclaves (40 rpm). After filtration with deionized water, obtained zeolite was dried at 80 °C in a forced convection oven. To remove organic template, the as-synthesized zeolite was calcined at 500 ℃ for 5 h under air flow. Calcined zeolite was ion-exchanged in 3 M ammonium chloride (NH_4Cl) solution at 60 °C for 8 times to obtain NH_4-RHO zeolite. Subsequently, NH_4^+-zeolites were ion exchanged with KNO_3 solution (10 wt.%) at 80 °C for 4 times to obtain K-RHO zeolite. The final zeolite was dried at 80 ℃ in a forced convection oven.

MER zeolite was synthesized as described in previous literature.[3] Tetraethylammonium hydroxide (TEAOH) solution (35 wt.%) and KOH were dissolved in deionized water. Then, aluminum hydroxide was added to the solution, being stirred until it becomes clear. Colloidal silica (Ludox, HS-40) was added to the clear solution, and final solution was aged at room temperature for 2 h. The final gel composition was 1.75 K_2O:Al_2O_3:10 SiO_2:4.4 TEAOH:130 H_2O. After transferring the solution to a Teflon-lined stainless-steel autoclave, hydrothermal synthesis was performed at 150 °C for 4 days while rotating the autoclaves (15 rpm). After filtration with deionized water, obtained zeolite was dried at 100 °C in a forced convection oven. To remove organic template, the as-synthesized zeolite was calcined at 600 °C for 6 h under air flow.

PAU zeolite was synthesized using embryonic seeds as described in previous literature.[4-5] PAU embryonic seeds were synthesized as follows. TEAOH solution (35 wt.%), NaOH and KOH were dissolved in deionized water. Then, aluminum hydroxide was added to the solution, being stirred until it becomes clear. Colloidal silica (SNOWTEX, ST-40) was added to the clear solution, and final solution was aged at room temperature for 2 h. The final gel composition was 0.9 Na_2O:0.4 K_2O:Al_2O_3:9 SiO_2:2.8 TEAOH:140 H_2O. After transferring the solution to a Teflon-lined stainless-steel autoclave, hydrothermal synthesis was performed at 120 °C for 5 days without rotation. After filtration with deionized water, obtained embryonic seeds were dried at 100 °C in a forced convection oven.

PAU zeolite was synthesized with the same gel composition as embryonic seeds synthesis. After aging at room temperature for 2 h, embryonic seeds were added to the solution. The solution was transferred to a Teflon-lined stainless-steel autoclave and hydrothermally treated at 140 °C for 2 days under rotation (15 rpm). After filtration with deionized water, obtained zeolite was dried at 100 °C in a forced convection oven. To remove organic template, the as-synthesized zeolite was calcined at 550 °C for 5 h under air flow. Calcined zeolite was ion-exchanged with NH_4NO_3 solution (3 M) for 6 times at 60 °C and subsequently with KNO_3 solution (10 wt.%) at 80 °C for 4 times to obtain K^+ form-PAU zeolite.

The chemical compositions of K^+-zeolites were measured with an inductively coupled plasma-atomic emission spectroscopy (ICP-AES, Galbraith Laboratories), which are summarized in Table S1.

H-RHO and H-PAU zeolites were obtained by calcining NH_4-RHO and NH_4-PAU at 500 °C for 5 h under air flow, respectively.

Powder X-ray diffraction

Powder X-ray diffraction patterns (PXRD) of K-RHO, K-MER and K-PAU zeolites were obtained with a MiniFlex (Rigaku) in 0.01° resolution and 5°/min scan rate. All measurement were performed *ex-situ*

under ambient environment.

Humid CO_2 adsorption analysis

We investigated humid CO_2 adsorption in zeolites with thermogravimetric analysis (TGA) and diffuse reflectance infrared Fourier transformed spectroscopy (DRIFTS). For humid environment, a 5.0 % (±0.5%) relative humidity (RH) was chosen to precisely investigate the competitive adsorption of water and CO_2 in zeolites without losing resolution as a result of water dominating the coadsorption event excessively at higher RH. This led us to insight about water-resilient CO_2 bonding sites in zeolites. Such sites also have a practical importance because they decrease the cycle time required during regeneration, in a kinetic separation that relies on the slower rates of water transport.

-Thermogravimetric analysis

TGA was conducted with a TGA Q5000 (TA instrument) to measure the CO_2 uptake under humid conditions. A 10-20 mg of zeolite sample was loaded on a platinum pan and dehydrated at 350 °C under 100 mL/min of air flow to measure a mass of zeolite (W_{dehy}). First step of TGA measurement (Step I) involves cooling the sample to 30 °C, and saturating with H_2O under humid air flow (5% (±0.5%) RH). The humid air flow was generated by passing through a water bubbler and mixed with dry air to make humid air flow with 5% RH at 30 °C. Once it reached equilibrium, the sample mass was measured (W_{H2O}). Subsequently, the humid air flow was switched to humid CO_2 (1 bar of CO_2) at the same RH and temperature (Step II), and equilibrated mass was measured to be $W_{H2O+CO2}$. After H_2O+CO_2 adsorption measurement, we switched from humid CO_2 to humid air again (Step III), at the same RH and temperature, to monitor the mass profile during CO_2 desorption.

For conventional quantification with TGA alone, the mass increase at the step I obviously indicates the amount of water adsorbed on the zeolite at the given relative humidity. In order to calculate the CO_2 uptake during humid CO_2 adsorption at step II, we invoke a heuristic that is conventionally used in the literatures,[6-8] which assumes the absence of change in the amount of pre-equilibrated water at step I after CO_2 adsorption at step II. Based on this heuristic, uptakes of water and CO_2 are calculated by following equations below.

$$\text{Water uptake (mmol/g)} = \frac{W_{H2O} - W_{dehy}}{W_{dehy}} \times \frac{1000}{18} \frac{\text{mmol of } H_2O}{\text{g}}$$

$$CO_2 \text{ uptake (mmol/g)} = \frac{W_{H2O+CO2} - W_{H2O}}{W_{dehy}} \times \frac{1000}{44} \frac{\text{mmol of } CO_2}{\text{g}}$$

Note that this quantification will be corrected with a DRIFT spectroscopy later to rigorously quantify H_2O and CO_2 uptake under humid CO_2 conditions since the heuristic is not always applicable.

-DRIFTS analysis

We conducted an *In-situ* DRIFTS with a Tensor 27 (Bruker) with a Mercury-Cadmium-Telluride (MCT) detector. The sample was loaded in a diffuse reflectance cell (Praying Mantis), and characterized under the same procedures as used in the thermogravimetric analysis described above. Background spectra of all DRIFTS data shown were spectra of zeolite samples themselves under air flow at 30 °C, after dehydration at 350 °C. With the spectra of dehydrated zeolites as a background, time-resolved spectra were obtained with a resolution of 1 cm^{-1}.

-Quantification of H_2O and CO_2 combining TGA and DRIFTS

All DRIFT spectra obtained under humid CO_2 environment were subtracted to a spectrum of gas phase CO_2 (15% CO_2 balanced with air) to eliminate the contribution of gas CO_2 in the IR spectra. Detailed procedures of this subtraction are described in Fig. S4 and S7 below (*vide infra*). The obtained

spectra after the subtraction were used to quantify H_2O and CO_2 amount in zeolites. Unlike the previous paper where we had used an IR band of H–O–H bending (δ) at 1800–1500 cm^{-1} to quantify it,[9] we herein turned to IR bands in near IR region of 5500–4800 cm^{-1} (combination band (ν+δ)) in order to avoid band interference presumably caused by a phase transition of zeolite structure during CO_2 adsorption (Fig. S6). Gallas et al.,[10] have proposed that integrated area of this IR band involves the same quantitative information for adsorbed H_2O as what H–O–H bending (δ) IR bands do. Integrated area of the IR band at 5500–4800 cm^{-1} refers to the amount of adsorbed H_2O in zeolites.[10] Therefore, the relative changes in the area of this IR band between under humid air conditions versus humid CO_2 conditions represent the relative amount of H_2O desorbed by CO_2 adsorption compared to water amount humid air conditions. Based on the H_2O uptake under humid air (5% RH, 30 °C) obtained via TGA above, we quantified the amount of H_2O desorbed (i.e. Relative change in the area $\times$ H_2O uptake (mmol/g) in TGA at step I). It led us to obtain "IR corrected" H_2O uptake under humid CO_2 conditions as following.

"IR corrected" H_2O uptake (mmol/g)

= "TGA only" H_2O uptake (mmol/g) - the amount of H_2O desorbed (mmol/g)

When H_2O was desorbed during humid CO_2 adsorption at step II, apparent mass increase at step II could not fully reflect the amount of CO_2 adsorption in the zeolites, thereby it caused underestimation on CO_2 uptake. In order to correct it, weight decrease that would have occurred due to the water desorption should be compensated as following.

"IR corrected" CO_2 uptake (mmol/g)

$$= \text{"TGA only" } CO_2 \text{ uptake (mmol/g)} + \text{the amount of } H_2O \text{ desorbed (mmol/g)} \times \frac{18\ g/mol_{H2O}}{44\ g/mol_{CO2}}$$

To monitor CO_2 adsorption via DRIFTS, we used IR bands at 2300–2250 cm^{-1}, which was assigned to the asymmetric stretching of $^{13}CO_2$ with a ~1% of natural abundance. The integrated area of $^{13}CO_2$ IR band at equilibrium (at the end of step II) should represent "IR corrected" humid CO_2 uptake above. During transient experiments in Fig. S9 when CO_2 adsorption was changing by time on stream, dynamic CO_2 uptakes were calculated based on relative area in $^{13}CO_2$ IR band compared to the area at the equilibrium. For dynamic H_2O uptakes, the same calculation was applied, using the IR band at 5500–4800 cm^{-1}.

-Procedure for the subtraction of IR spectra: Normalization with gas CO_2 spectrum.

Since IR absorbance from gas phase CO_2 is so huge, its IR signals make it difficult to identify and characterize the IR bands from chemical substances on the surface. Therefore, we subtracted its IR bands from our data to eliminate its contribution to the resulting spectra. For the subtraction, we selected IR bands of gas phase CO_2 centered at 3729 cm^{-1} to normalize the spectra, which corresponded to R branch of $\nu_1+\nu_3$ combination band of CO_2. It was because i) it had a moderate intensity (i.e. not too weak and not too strong), which was suitable for the normalization, and ii) it was the IR band that was least overlapped with other IR bands from zeolites and H_2O. We measured intensity of this band from the background drawn from the linear line from 3753 cm^{-1} to 3714 cm^{-1}, as shown in Fig. S4a and subtracted two spectra after normalization based on measured IR band intensity at 3729 cm^{-1}. Example of resulting spectrum is exhibited in Fig. S4b, and demonstrates that the contribution from gas phases CO_2 is successfully eliminated. After subtraction, we were able to extract sole –OH stretching bands of water under humid CO_2 conditions (5% RH), while small IR bands from physisorbed CO_2 on zeolites (showing small peak at around 3700 cm^{-1} and 3620 cm^{-1}) still remains but were not significantly disturbing due to their relatively low intensities. The spectra were exhibited after being transformed to Kubelka-Munk scale.

-Procedure for the subtraction of IR spectra: Deleting a gas phase CO_2 contribution in near IR region.

In spectral region of 5500-4800 cm^{-1} that includes the combination band of H_2O in zeolites, multiple IR bands from gas phase CO_2 were also present and interfered with those IR bands of H_2O. Since their intensities were too small to be subtracted via the normalization approach, we instead removed the signals from 5132 cm^{-1} to 5043 cm^{-1}, from 5016 cm^{-1} to 4922 cm^{-1}, and from 4885 cm^{-1} to 4814 cm^{-1} where the IR bands of gas phase CO_2 were present, and connected each end with linear lines to remove the contribution from gas phase CO_2 (red line in Fig. S7a). Example of resulting spectrum is shown in Fig. S7b. The area of corresponding IR band was integrated after this data processing.

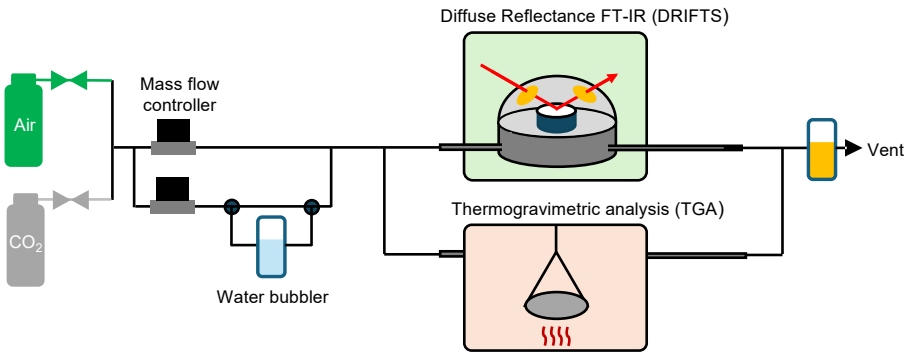

Scheme S1. A schematic of DRIFTS and TGA apparatus with flow systems for humid CO_2 adsorption experiment.

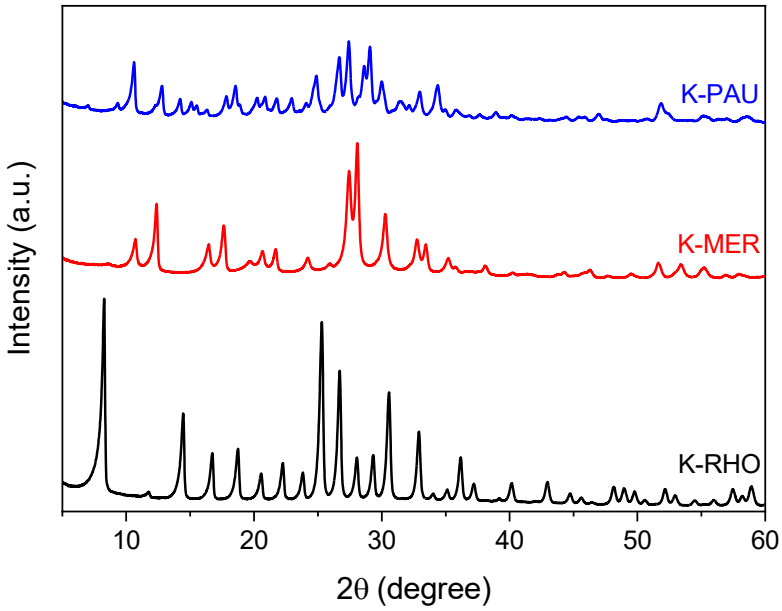

Fig. S1. PXRD data of K-RHO, K-MER and K-PAU zeolites.

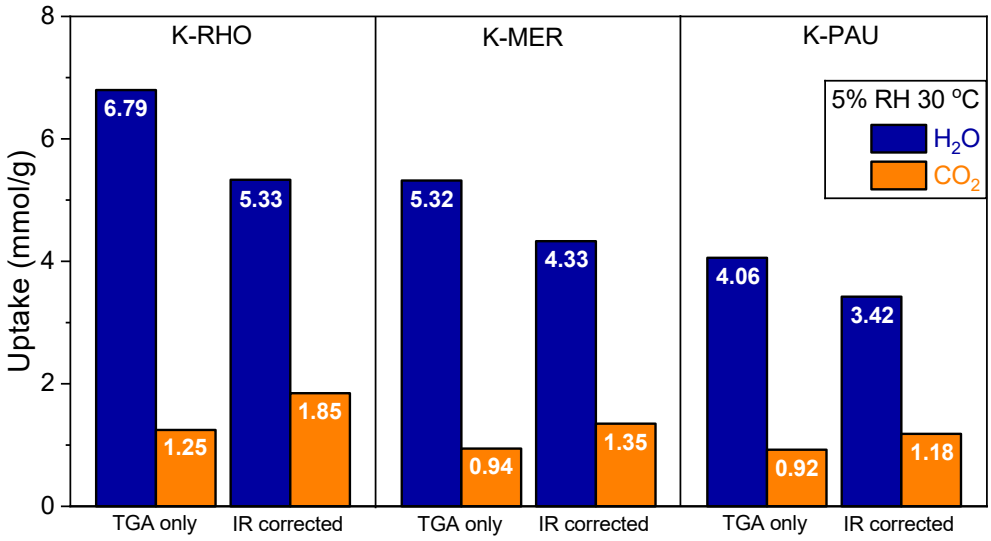

Fig. S2. Quantification results of H_2O and CO_2 in K-RHO, K-MER and K-PAU at 5% RH, 30 °C. "TGA only" refers to the results calculated from TGA alone, and "IR corrected" refers to the results calculated from the combination of TGA and DRIFTS.

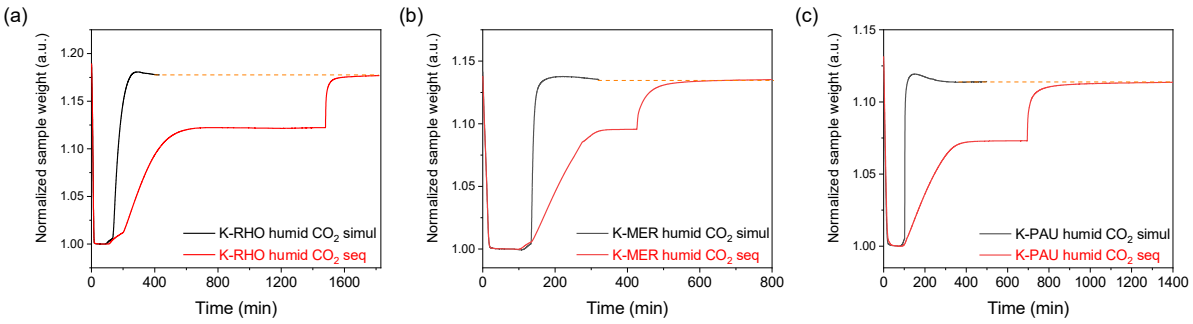

Fig. S3. TGA profiles of (a) K-RHO, (b) K-MER and (c) K-PAU during H_2O and humid CO_2 adsorption when two gas components are adsorbed simultaneously (black) and sequentially (red, H_2O first, then subsequent humid CO_2 adsorption) under 5% RH at 30 ^oC. The data are normalized with the sample weights at 350 ^oC, which correspond to the weight of dehydrated zeolites.

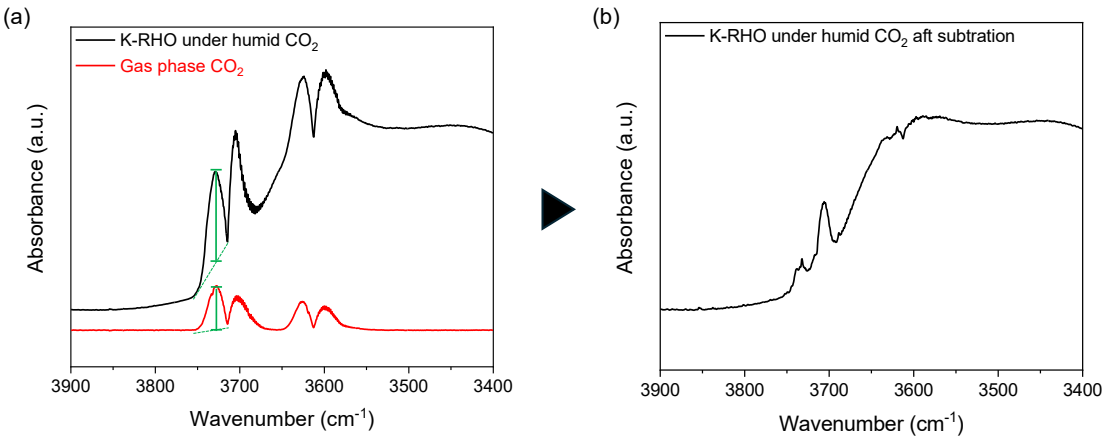

Fig. S4. (a) DRIFT spectra of K-RHO under humid CO_2 conditions (black, 5% RH and 30 ^oC) and gas phase CO_2 measured with KBr (red). Green lines demonstrate the approach to measure intensity of IR band at 3729 cm^{-1}. (b) DRIFT spectrum of K-RHO under humid CO_2 conditions (5% RH and 30 ^oC) after subtraction to the spectrum of gas phase CO_2, normalizing both spectra with the measured IR band intensity at 3729 cm^{-1}.

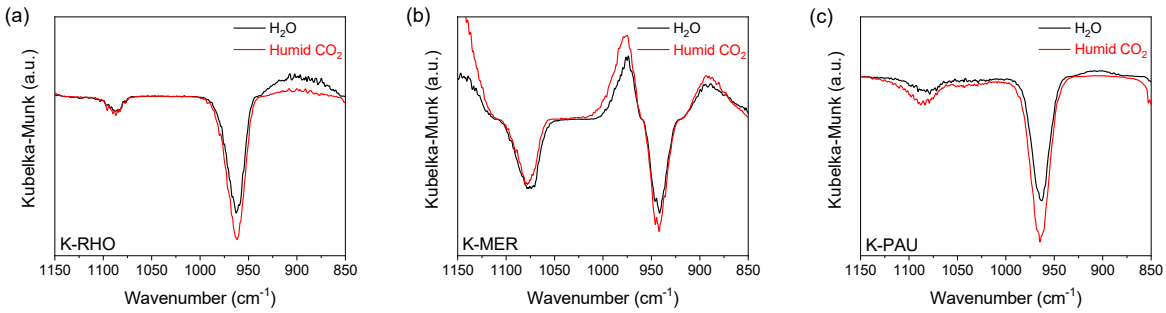

Fig. S5. DRIFT spectra of T-O-T vibration in (a) K-RHO, (b) K-MER and (c) K-PAU under humid air (black, H_2O) and humid CO_2 conditions (red, Humid CO_2).

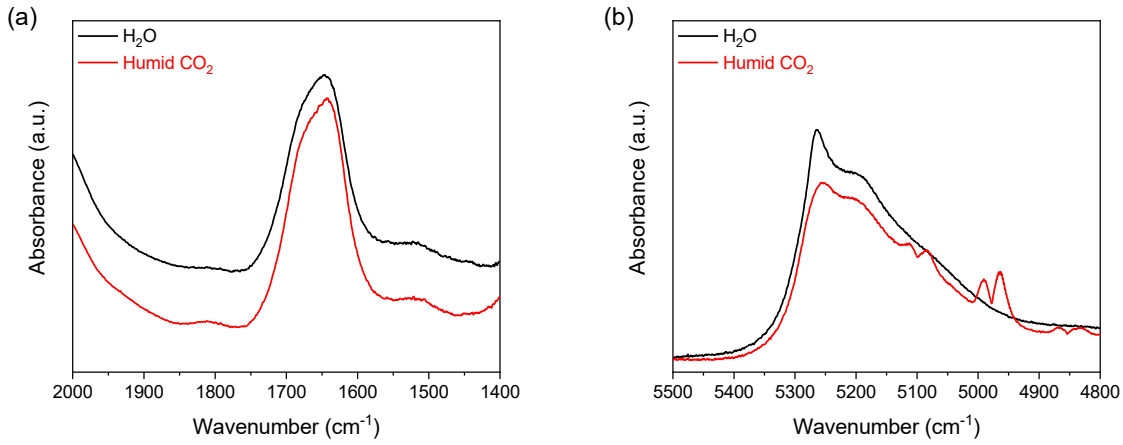

Fig. S6. (a) DRIFT spectra at 2000-1400 cm^{-1} of K-RHO zeolite under humid air and humid CO_2 conditions at 5% RH and 30 °C. (b) DRIFT spectra at 5500-4800 cm^{-1} of K-RHO zeolite under humid air and humid CO_2 conditions at 5% RH and 30 °C. All data shown here are in absorbance scale without any spectrum subtraction.

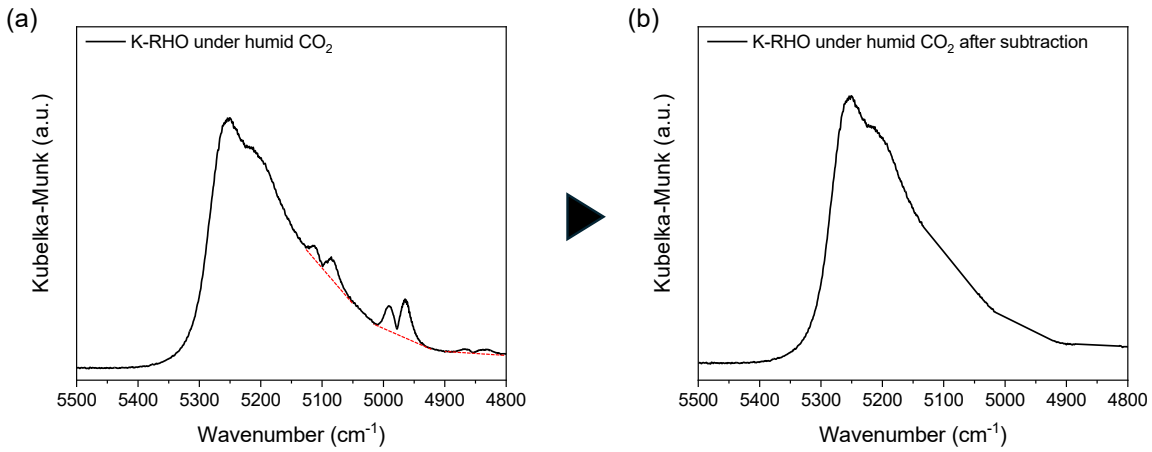

Fig. S7. (a) DRIFT spectra of K-RHO under humid CO_2 conditions (5% RH and 30 ^oC). Red lines demonstrate the approach to subtract the contribution from gas phase CO_2. (b) DRIFT spectrum of K-RHO under humid CO_2 conditions (5% RH and 30 ^oC) after the corresponding subtraction.

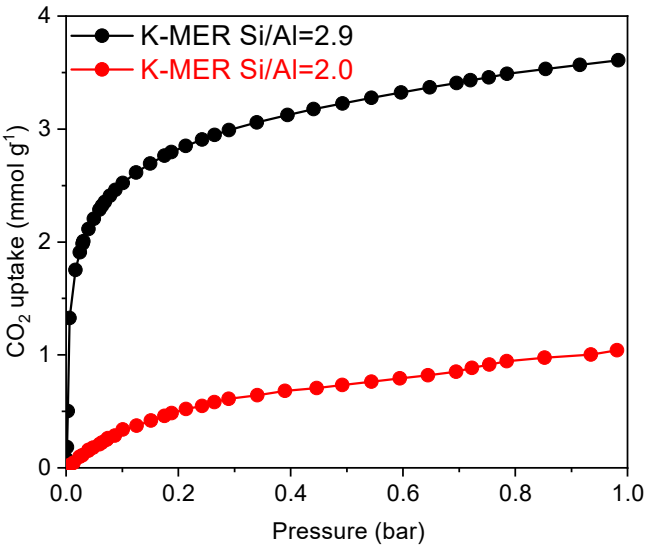

Fig. S8. Dry CO_2 isotherms of K-MER Si/Al=2.9 (in this study) and K-MER Si/Al=2.0 (previous study[9]) at 30 °C.

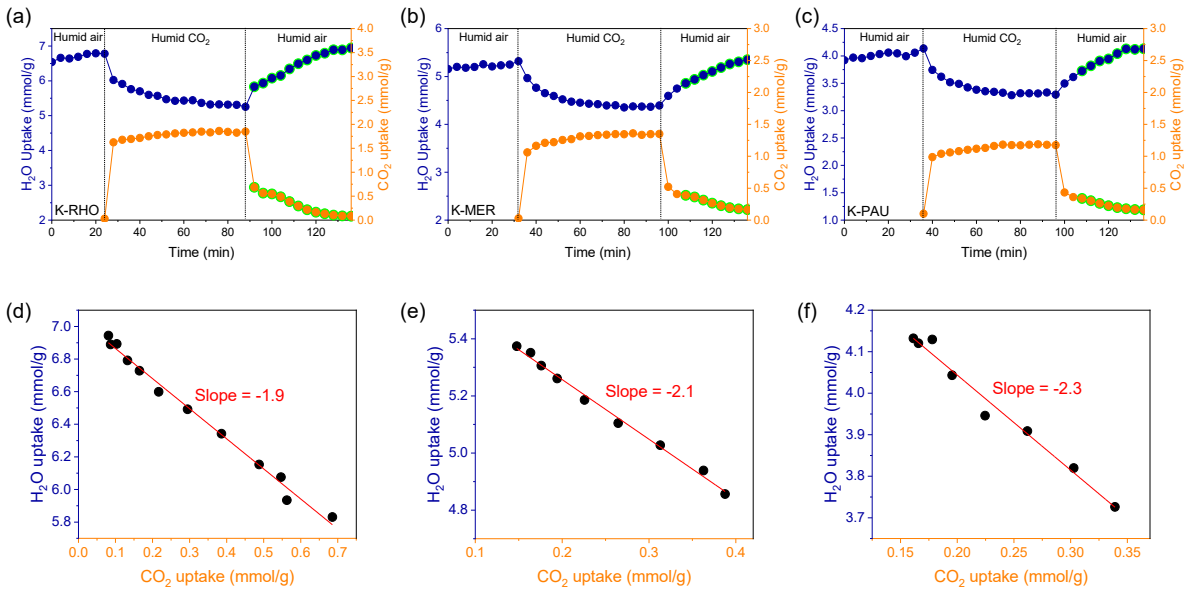

Fig. S9. (a-c) Time-resolved profiles for the amount of adsorbed water and CO_2 in (a) K-RHO, (b) K-MER and (c) K-PAU during humid CO_2 adsorption/desorption at 30 °C under 5% RH. Blue circles represent adsorbed water (mmol/g), and orange circles represent adsorbed CO_2 (mmol/g). (d-f) Parametric plots representing the amount of adsorbed water and CO_2 in (d) K-RHO, (e) K-MER and (f) K-PAU during step III (desorption under humid air). The datapoints were chosen from Fig. S9a, b and c, respectively, shown in green coloration in these figures.

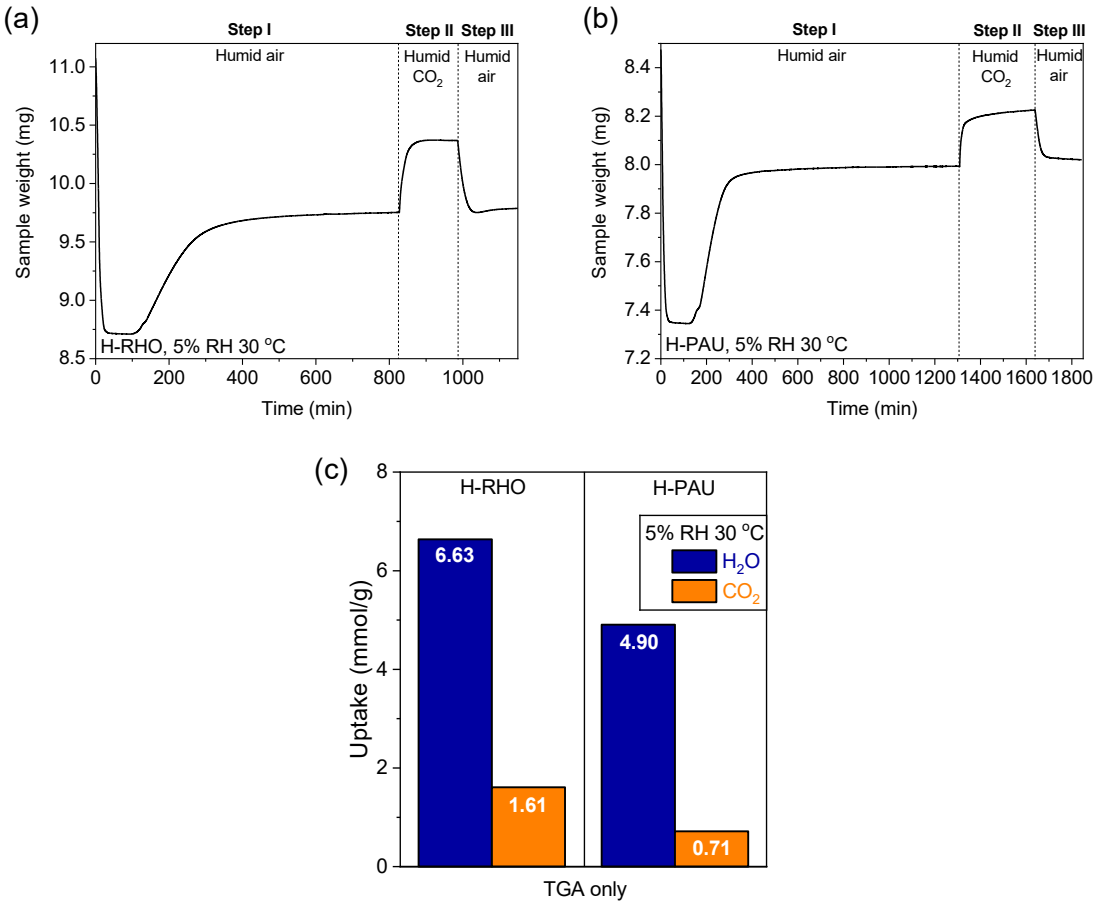

Fig. S10. (a) TGA profiles of (a) H-RHO, (b) H-PAU zeolites during gas adsorption under humid air (step I), humid CO_2 (step II) and humid air (step III) conditions at fixed 5% RH and 30 °C. (c) Quantification results of H_2O and CO_2 in H-RHO an H-PAU during humid CO_2 adsorption, calculated based on the data in Fig. S10a and b, respectively.

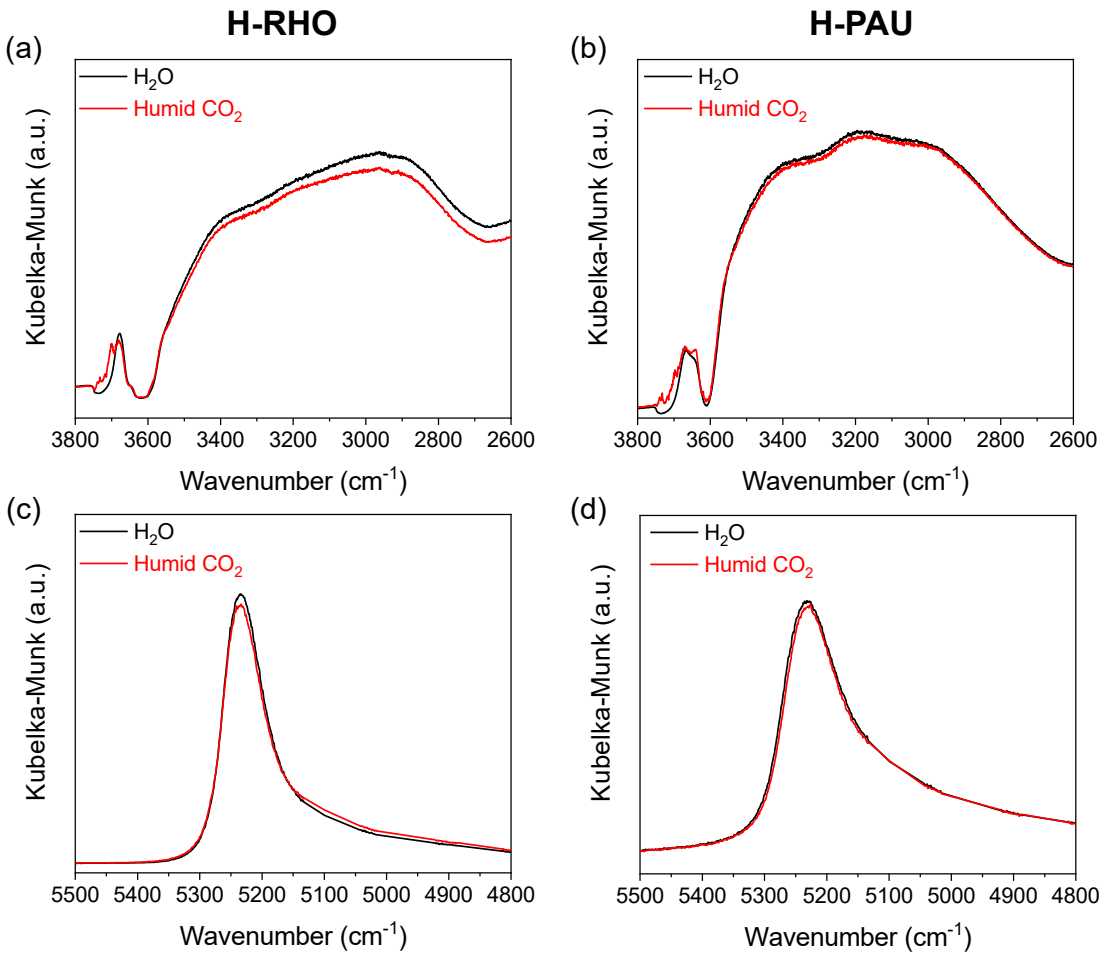

Fig. S11. (a, b) DRIFT spectra of –OH stretching IR band from adsorbed H_2O in H-RHO and H-PAU, respectively, after equilibrated under humid air (H_2O, black) and subsequent humid CO_2 conditions (Humid CO_2, red) at 5% RH and 30 °C. (c, d) DRIFT spectra of combination IR band of H_2O in H-RHO and H-PAU, respectively, under the same conditions.

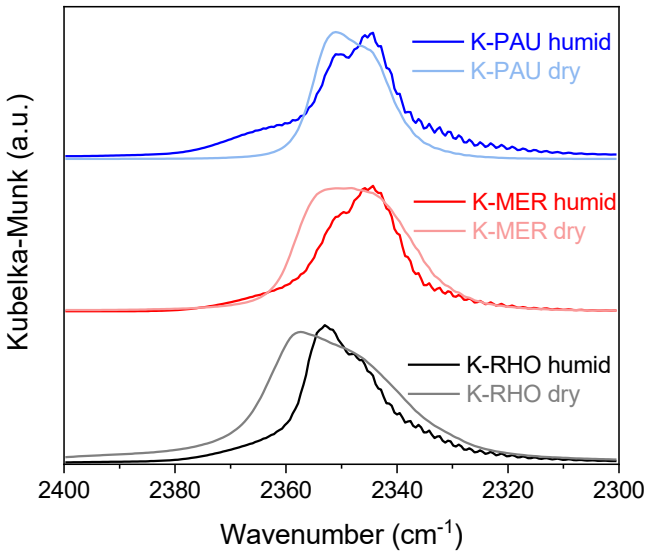

Fig. S12. DRIFT spectra of adsorbed CO_2 in K^+-D8R zeolites (K-RHO, K-MER and K-PAU) under humid and dry CO_2. The spectra were obtained during CO_2 desorption under humid air conditions at 5% RH and dry air conditions, respectively, at 30 ^oC after CO_2 adsorption at the same conditions.

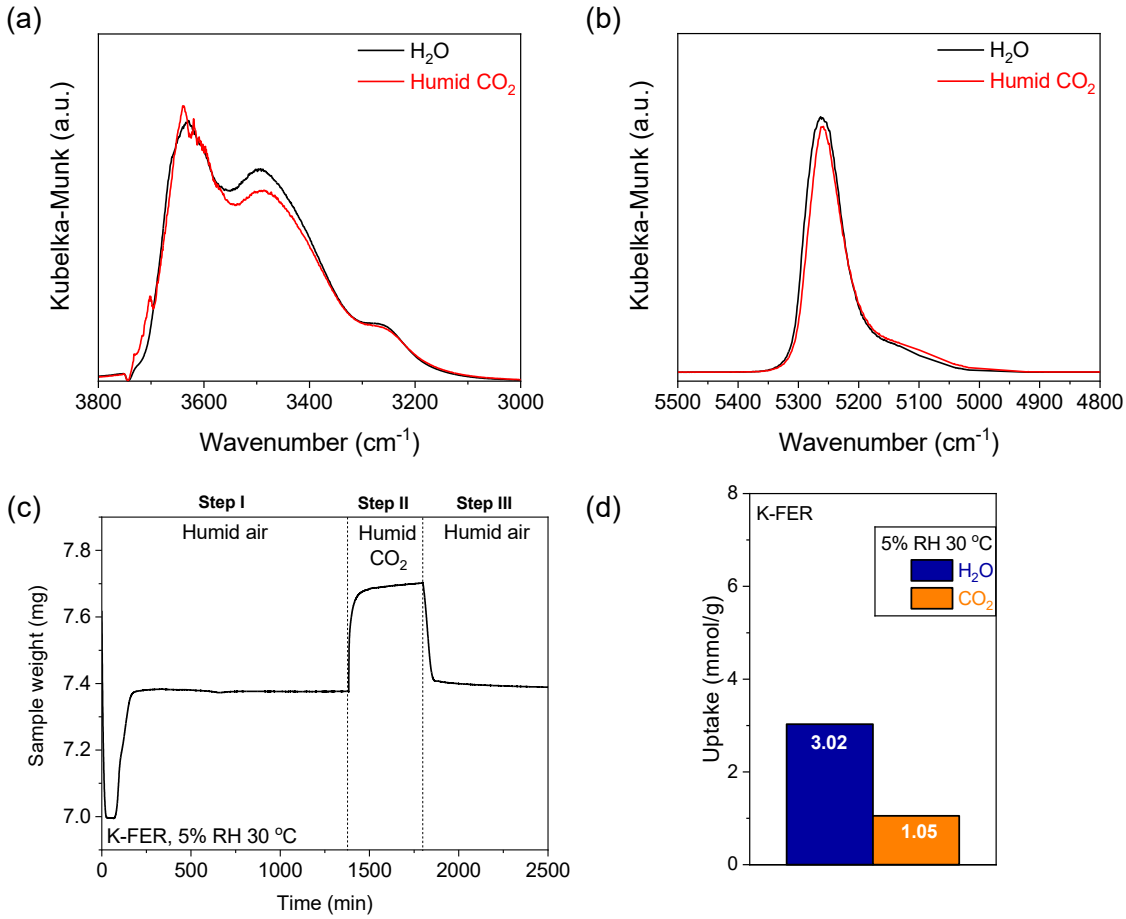

Fig. S13. DRIFT spectra of (a) –OH stretching IR band and (b) combination IR band from adsorbed H_2O in K-FER after equilibrated under humid air (H_2O, black) and subsequent humid CO_2 conditions (Humid CO_2, red) at 5% RH and 30 °C. (c) TGA profiles of K-FER zeolite during gas adsorption under humid air (step I), humid CO_2 (step II) and humid air (step III) conditions at fixed 5% RH and 30 °C. (d) Quantification results of H_2O and CO_2 in K-FER during humid CO_2 adsorption, calculated based on the data in Fig. S13c.

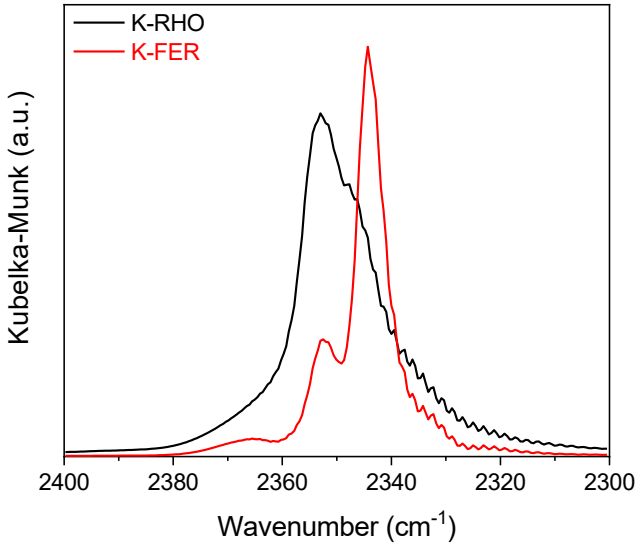

Fig. S14. DRIFT spectrum of adsorbed CO_2 in K-FER zeolite, and its comparison with the spectrum of K-RHO. The spectra were obtained during CO_2 desorption under humid air conditions at 5% RH and 30 °C after humid CO_2 adsorption at the same conditions.

Table S1. ICP-AES results of K-RHO, K-MER and K-PAU zeolites

	K (wt.%)	Si (wt.%)	Al (wt.%)	Si/Al[a]	K^+/Al[a]
K-RHO	9.6	26.4	6.9	3.7	0.97
K-MER	11.8	26.2	8.6	2.9	0.95
K-PAU	9.6	27.9	7.4	3.6	0.90

[a] molar ratio

References

(1) Chatelain, T.; Patarin, J.; Fousson, E.; Soulard, M.; Guth, J.; Schulz, P., Synthesis and characterization of high-silica zeolite RHO prepared in the presence of 18-crown-6 ether as organic template. *Microporous Materials* **1995,** *4* (2-3), 231-238.

(2) Palomino, M.; Corma, A.; Jorda, J. L.; Rey, F.; Valencia, S., Zeolite Rho: a highly selective adsorbent for CO2/CH4 separation induced by a structural phase modification. *Chem. Comm. (Camb)* **2012,** *48* (2), 215-7.

(3) Georgieva, V. M.; Bruce, E. L.; Verbraeken, M. C.; Scott, A. R.; Casteel, W. J., Jr.; Brandani, S.; Wright, P. A., Triggered Gate Opening and Breathing Effects during Selective CO2 Adsorption by Merlinoite Zeolite. *J. Am. Chem. Soc.* **2019,** *141* (32), 12744-12759.

(4) Shu Hikima, R. O., Noriko Katagiri, Takahiko Takewaki MANUFACTURING METHOD OF ZEOLITE. JP2023114891, 2023.

(5) Shu Hikima, R. O., Noriko Katagiri, Takahiko Takewaki ZEOLITE, METHOD OF ADSORBING CARBON DIOXIDE, METHOD OF SEPARATING CARBON DIOXIDE, DEVICE OF ADSORBING/SEPARATING CARBON DIOXIDE, AND METHOD OF PRODUCING ZEOLITE. JP2023114890, 2023.

(6) Sánchez-González, E.; Álvarez, J. R.; Peralta, R. A.; Campos-Reales-Pineda, A.; Tejeda-Cruz, A.; Lima, E.; Balmaseda, J.; González-Zamora, E.; Ibarra, I. A., Water adsorption properties of NOTT-401 and CO2 capture under humid conditions. *ACS omega* **2016,** *1* (2), 305-310.

(7) Peralta, R. A.; Alcántar-Vázquez, B.; Sánchez-Serratos, M.; González-Zamora, E.; Ibarra, I. A., Carbon dioxide capture in the presence of water vapour in InOF-1. *Inorg. Chem. Front.* **2015,** *2* (10), 898-903.

(8) Alvarado-Alvarado, D.; González-Estefan, J. H.; Flores, J. G.; Álvarez, J. R.; Aguilar-Pliego, J.; Islas-Jácome, A.; Chastanet, G.; González-Zamora, E.; Lara-García, H. A.; Alcántar-Vázquez, B., Water adsorption properties of Fe (pz)[Pt (CN) 4] and the capture of CO2 and CO. *Organometallics* **2020,** *39* (7), 949-955.

(9) Lee, H.; Xie, D.; Zones, S. I.; Katz, A., CO2 Desorbs Water from K-MER Zeolite under Equilibrium Control. *J. Am. Chem. Soc.* **2023,** *146* (1), 68-72.

(10) Gallas, J.-P.; Goupil, J.-M.; Vimont, A.; Lavalley, J.-C.; Gil, B.; Gilson, J.-P.; Miserque, O., Quantification of water and silanol species on various silicas by coupling IR spectroscopy and in-situ thermogravimetry. *Langmuir* **2009,** *25* (10), 5825-5834.